

STEREO / IMPACT / SEPT: The Particle Investigation CMAD

| Revision | Effective Date | Description of Changes |
|------------|----------------|----------------------------------|
| Baseline | 05/19/2021 | First tracked version |
| Revision 1 | 04/27/2026 | Formatting and minor corrections |

1. Overview

The Solar Electron and Proton Telescope (SEPT), part of the IMPACT investigation onboard the STEREO spacecraft, were designed and built by the Institut für Experimentelle und Angewandte Physik, Christian-Albrechts-Universität Kiel, Germany by R. Mueller-Mellin, in co-operation with ESA. After successful commissioning, SEPT started its scientific observations in mid December 2006.

SEPT consists of two dual double-ended magnet/foil particle telescopes which cleanly separate and measure electrons in the energy range from 30–400 keV and protons from 60–7 000 keV. Anisotropy information on a non-spinning spacecraft is provided by the two separate telescopes: SEPT-E looking in the ecliptic plane along the Parker spiral magnetic field both towards and away from the Sun, and SEPT-NS looking vertical to the ecliptic plane towards North and South. The dual set-up refers to two adjacent sensor apertures for each of the four view directions: one for protons, one for electrons. The double-ended set-up refers to the detector stack with view cones in two opposite directions: one side (electron side) is covered by a thin foil, the other side (proton side) is surrounded by a magnet. The thin foil leaves the electron spectrum essentially unchanged but stops low energy protons. The magnet sweeps away electrons but lets ions pass.

At the time of solar superior conjunction in July 2015 the spacecraft were rotated, and the SEPT-E telescopes are no longer looking along the Parker spiral. Namely, all telescopes are oriented perpendicular to the Parker spiral. This orientation strongly limits the pitch angle coverage of the SEPT instrument. The consequence is, that if particles beams streaming from the Sun arrive at STEREO, the measured intensities are lower and the onset times of SEPs are not correctly measured. Specifically, the onset is delayed in comparison to the true onset.

1.1. Heritage

The STEREO IMPACT/SEPT is an originally designed instrument and were built under the direction of Reinhold Mueller-Mellin (Mueller-Mellin et al. 2008). The Solar Electron and Proton Telescope (SEPT) has two solid state detectors (SSDs) which are

operated in anti-coincidence. One SSD looks through an absorption foil and its partner through the air gap of a magnet system. The foil leaves the electron spectrum essentially unchanged but stops protons of energy up to the energy of electrons (~400 keV) which penetrate the SSD. The magnet is designed to sweep away electrons below 400 keV, but leaves ions unaffected. Electrons are registered in the energy range 35 – 450 keV with a nominal geometrical factor for the foil telescope of 0.13 cm² sr. Protons are registered in the energy range 65 – 6500 keV with a geometrical factor for the magnet telescope of 0.17 cm² sr. The main parameters of SEPT are presented in the **Table 1**

Table 1- IMPACT /SEPT characteristics

| Description | Electrons | Protons |
|---|-----------------------------|-----------------------------|
| Energy interval | 30–400 keV | 60–7 000 keV |
| Field of view | 4 × 52.8° | 4 × 52.0° |
| Geometrical factor (4x -four telescopes) | 4 × 0.13 cm ² sr | 4 × 0.17 cm ² sr |
| Channels | 32 | 32 |

1.2.Product Description

The SEPT produces three data sets: the scientific data product (1) from the two telescopes SEPT-E and SEPT-NS are comprised in a total of 8 histograms with 32 bins each. Four electron histograms (one for each of four directions) cover the electron energy range from 30 keV to 400 keV with quasi-logarithmic binning. Four proton histograms (one for each of four directions) cover the proton energy range from 60 keV to 2 MeV with quasi-logarithmic binning and a single bin for ions from 2–7 MeV/n. All histogram data are logarithmically compressed using a 24-bit to 14-bit compression scheme.

(2) a beacon product: electron and proton rates in four energy channels for each species for continuous transmission of beacon mode data to the ground station. The lowest and highest energy channels are sectorized in the four look directions while the two mid-range rates are summed over the four look directions. This results in a total of 20 rates shown in **Table 2**, which are compressed using a 24-to-16 bit compression scheme for transmission. The time resolution is 60 seconds.

(3) Housekeeping data.

Table 2 - SEPT beacon mode data

| Species | Energy window [keV] | Geom. factor [cm ² sr] |
|-----------------------|---------------------|-----------------------------------|
| Electrons | 35 - 65 | 0.13 |
| Electrons | 65 - 125 | 0.52 |
| Electrons | 125 - 255 | 0.52 |
| Electrons | 255 - 485 | 0.13 |
| Ions (mostly protons) | 75 - 137 | 0.17 |
| Ions (mostly protons) | 137 - 623 | 0.68 |
| Ions (mostly protons) | 623 - 2 224 | 0.68 |
| Ions (mostly protons) | 2 224 - 6 500 | 0.17 |

SEPT units generate counting rates with 1min cadence and 32 energy bins for each viewing direction. Level 2 data files are produced regularly at the University of Kiel using the latest calibration data available and organized in daily files in ASCII format with different temporal averages (1 minute, 10 minutes, 1 hour and 1 day). The data files are publicly available in the following URL: <http://www2.physik.uni-kiel.de/stereo/data/sept/level2/>. Level 2 data include several corrections not available for the level-1 CDF data files: differential non-linearity correction, energy-dependent electron geometric factors and efficiency corrections (particularly important for the sunward-pointing electron telescope onboard STEREO-A, which shows lower detection efficiency than the other telescopes). In addition, those channels not containing scientifically useful data have been removed.

Table 3. Contents of SEPT level 2 ion data files

| Item | Data type | Content |
|------|------------------------|---|
| 1 | Double-precision float | Timestamp corresponding to the center of the accumulation interval, expressed as Julian date (Julian date 0.0 is Jan. 1, 4713 B.C. at 12:00:00) |
| 2 | Integer | Year |

IMPACT / SEPT Calibration and Measurement Algorithm Document

| | | |
|----------|---------|---|
| 3 | Float | Fractional day of year |
| 4 | Integer | Hour of day |
| 5 | Integer | Minute of hour |
| 6 | Integer | Second of minute |
| 7 to 36 | Float | Ion intensities for energy bins 02 to 31 given in $\text{cm}^{-2} \text{s}^{-2} \text{sr}^{-1} \text{MeV}^{-1}$ |
| 37 to 66 | Float | Statistical uncertainties of ion intensities for energy bins 02 to 31, given in $\text{cm}^{-2} \text{s}^{-1} \text{sr}^{-1} \text{MeV}^{-1}$ |
| 67 | Float | Accumulation time in seconds. Currently this does not include dead-time corrections |

Table 4. Contents of SEPT level 2 electron data files

| Item | Data type | Content |
|------|------------------------|---|
| 1 | Double-precision float | Timestamp corresponding to the center of the accumulation interval, expressed as Julian date (Julian date 0.0 is Jan. 1, 4713 B.C. at 12:00:00) |
| 2 | Integer | Year |
| 3 | Float | Fractional day of year |
| 4 | Integer | Hour of day |
| 5 | Integer | Minute of hour |
| 6 | Integer | Second of minute |

| | | |
|----------|-------|--|
| 7 to 21 | Float | Electron intensities for energy bins 02 to 16 given in $\text{cm}^{-2} \text{s}^{-1} \text{sr}^{-1} \text{MeV}^{-1}$ |
| 22 to 36 | Float | Statistical uncertainties of electron intensities for energy bins 02 to 16, given in $\text{cm}^{-2} \text{s}^{-1} \text{sr}^{-1} \text{MeV}^{-1}$ |
| 37 | Float | Accumulation time in seconds. Currently this does not include dead-time corrections |

The SEPT Level1, 1-minute data are available in CDF format, from the STEREO IMPACT Data center at Berkeley: http://stereo.ssl.berkeley.edu/L1_data.html and from CDAWeb.

2. Error Analysis and Corrections

Description of the data processing sequence.

For each SEPT telescope the starting point of the data processing is an array “counts” of $(32, n)$ elements, which correspond to the counts accumulated in 32 onboard channels. Such array is provided with a cadence of 1 minute, with a total of n elements (i.e. for one day of data the maximum expected value of n would be 1440). The ordered sequence of steps for the processing of these raw data in order to obtain calibrated level 2 data is described below.

3.1 Statistical errors

The counting rates observed by SEPT are expected to follow a Poisson distribution, therefore if N_i counts are accumulated in a certain counting interval for certain channel i , the statistical uncertainty is given by the square root of the number of counts:

$$\Delta N_i = \sqrt{N_i}$$

In order to obtain the statistical error for the calibrated intensities, these statistical uncertainties can be propagated quadratically through all the calculation steps described above.

3.2. Differential non-linearity correction

The onboard Analog-to-Digital Converters (ADC) deviate from the ideal response and a pulse that would correspond to a certain energy channel has some probability of being registered in the adjacent ones. This effect has been characterized on ground for the different SEPT units and can be mitigated using a matrix multiplication of the form (IDL syntax):

```
cc = matrix_multiply(dnlmatrix,c)
```

Where “c” is an array of 32 elements containing the counts registered in each bin at a given time, “dnlmatrix” is a 32x32 square matrix and “cc” is the corrected array of counts. The DNL correction matrices are different for each specific pdf electronics (16 matrices in total, attached to this document. These matrices are nearly diagonal; therefore, this correction is relatively small. Note that the matrix files use the following naming convention: fmSU_mN, where S is 1 for STEREO-A and 2 for STEREO-B, U is e for ecliptic and n” for north-south and N is 0, 1, 2, 3 for pdf0, pdf1, pdf2 and pdf3, respectively.

3.3. Calibration and efficiency correction

The particle intensities in physical units for each energy channel “i” are related to the counting rates by:

$$j_i = \frac{N_i}{g_i \Delta E_i \Delta t}$$

Where j_i is the intensity (or differential flux) in particles/(cm² s sr MeV), g_i is the geometric factor, $\Delta E_i = E_i^{low} - E_{i+1}^{low}$ is the width of the energy channel i in MeV and Δt is the accumulation time, which has a nominal value of 59.5938 s. The values of the energy borders and the geometric factors for electrons and ions are listed in Table 1. Note that electron channels above 425 keV contain data which are not useful for scientific analysis and should be discarded.

Moreover, an efficiency factor e_i can be introduced for each channel, mainly to correct the effect of the energy thresholds for the lowest energy channels:

$$j_i = \frac{N_i}{e_i g_i \Delta E_i \Delta t}$$

Table 5 Energy borders and geometric factors for the SEPT electron and ion telescopes

| Channel | Electron g_i (cm ² s sr) | Ion g_i (cm ² s sr) | Electron E_i^{low} (keV) | Ion E_i^{low} (keV) |
|---------|--|-------------------------------------|-------------------------------|--------------------------|
| 0 | 0.027 | 0.17 | 5.0 | 49.5 |
| 1 | 0.085 | 0.17 | 35.0 | 75.4 |
| 2 | 0.089 | 0.17 | 45.0 | 84.1 |

IMPACT / SEPT Calibration and Measurement Algorithm Document

| | | | | |
|----|-------|------|-------|-------------------|
| 3 | 0.095 | 0.17 | 55.0 | 92.7 |
| 4 | 0.101 | 0.17 | 65.0 | 101.3 |
| 5 | 0.101 | 0.17 | 75.0 | 110.0 |
| 6 | 0.106 | 0.17 | 85.0 | 118.6 |
| 7 | 0.108 | 0.17 | 105.0 | 137.0 |
| 8 | 0.113 | 0.17 | 125.0 | 155.8 |
| 9 | 0.109 | 0.17 | 145.0 | 174.6 |
| 10 | 0.110 | 0.17 | 165.0 | 192.6 |
| 11 | 0.114 | 0.17 | 195.0 | 219.5 |
| 12 | 0.112 | 0.17 | 225.0 | 246.4 |
| 13 | 0.113 | 0.17 | 255.0 | 273.4 |
| 14 | 0.095 | 0.17 | 295.0 | 312.0 |
| 15 | 0.074 | 0.17 | 335.0 | 350.7 |
| 16 | 0.054 | 0.17 | 375.0 | 389.5 |
| 17 | N/A | 0.17 | 425.0 | 438.1 |
| 18 | N/A | 0.17 | N/A | 496.4 |
| 19 | N/A | 0.17 | N/A | 554.8 |
| 20 | N/A | 0.17 | N/A | 622.9 |
| 21 | N/A | 0.17 | N/A | 700.7 |
| 22 | N/A | 0.17 | N/A | 788.3 |
| 23 | N/A | 0.17 | N/A | 875.8 |
| 24 | N/A | 0.17 | N/A | 982.8 |
| 25 | N/A | 0.17 | N/A | 1111.9 |
| 26 | N/A | 0.17 | N/A | 1250.8 |
| 27 | N/A | 0.17 | N/A | 1399.7 |
| 28 | N/A | 0.17 | N/A | 1578.4 |
| 29 | N/A | 0.17 | N/A | 1767.0 |
| 30 | N/A | 0.17 | N/A | 1985.3 |
| 31 | N/A | 0.17 | N/A | 2223.6 (6500.) |

The efficiency factors were obtained from the analysis of the first flight data, assuming a power-law spectral shape during SEP enhancements. They are very close to unity except for the first four energy channels. These channels should not be used for serious scientific analysis (especially the two lowest).

The values of the efficiencies for each SEPT telescope are provided in Table 2. The corresponding processing code would be:

```
FOR chan=0,31 DO BEGIN
    factor[chan,*]= dt*bw[chan]*g[chan]*eff[chan]
END FOR

j = correctedcounts/factor
```

where g is the geometric factor, dt the accumulation time, bw is the energy bin width ($\Delta E_i = E_i^{\text{low}} - E_{i+1}^{\text{low}}$) and eff is the efficiency.

Table 6 Array of efficiencies for the STEREO-A/SEPT telescopes

| Telescope | Array of 32 efficiencies |
|--------------|---|
| STA_E_e_Asun | 0.00011,0.102,0.622,1.03,1 |
| STA_E_p_Sun | 0.00008,0.067,0.606,1.227,1 |
| STA_E_e_Sun | 0.01104,0.629,1.007,0.999,1 |
| STA_E_p_Asun | 0.00337,0.473,1.188,1.039,1 |
| STA_e_North | 0.00002,0.002,0.44,1.028,1 |
| STA_P_South | 0.00439,0.687,1.184,0.992,1 |
| STA_e_South | 0.00008,0.090,0.736,1.281,1.128,1 |
| STA_p_North | 0.00046,0.513,1.156,1.024,1 |

Table 7 Array of efficiencies for the STEREO-B/SEPT telescopes

| Telescope | Array of 32 efficiencies |
|-------------|---|
| STB_e_Sun | 0.00049,0.192,0.954,1.04,1 |
| STB_p_Asun | 0.00009,0.265,0.959,1.155,1 |
| STB_e_Asun | 0.00012,0.169,0.769,1.013,1 |
| STB_p_Sun | 0.00019,0.00018,0.319,1.003,1 |
| STB_e_South | 0.00012,0.348,1.037,1.01,1 |
| STB_p_North | 0.01614,0.778,1.212,0.966,1 |
| STB_e_North | 0.00010,0.205,0.899,0.989,1 |
| STB_p_South | 0.00027,0.369,1.112,1.053,1 |

3.4. Additional efficiency correction for STA-Sun electron telescope

The cross-calibration procedures of the different SEPT telescopes during the decay phase of SEP events (when isotropy is expected) showed that the sunward pointing electron telescope onboard STEREO-A registered systematically lower counting rates compared with the other three apertures. In order to correct from this effect of unknown origin, an additional efficiency correction was introduced. The fluxes for this telescope are corrected by:

$$j = j/eff2$$

where j is the array of [32,n] intensities and $eff2$ is the following array of 32 elements:

```
eff2=[ 0.600, 0.643, 0.684, 0.717, 0.745, 0.770, 0.800,
0.835, 0.865, 0.890, 0.917, 0.945, 0.970, 0.994, 1.000, 1.000,
1.000, 1.000, 1.000, 1.000, 1.000, 1.000, 1.000, 1.000, 1.000,
1.000, 1.000, 1.000, 1.000, 1.000, 1.000, 1.000, 1.000]
```

4. In-flight inter-calibration and validation

SEPT data validation and the inter-calibration was done when the STEREO spacecraft were close to the Earth and to the ACE spacecraft by observation of SEPs during 23-24 January 2007 events (See Fig. 1).

Measurements at all three spacecraft show very comparable electron intensities and time profiles in the energy range 71-112 keV (Lario et al. 2013). There are some small differences in time profiles between STEREO and ACE observations which are caused by small different energy ranges, local magnetic field distribution and FOVs. The electron peak intensities between STEREO-A and STEREO-B are different by factor 1.1. The difference between the two STEREO s/c and ACE are by factor 1.3.

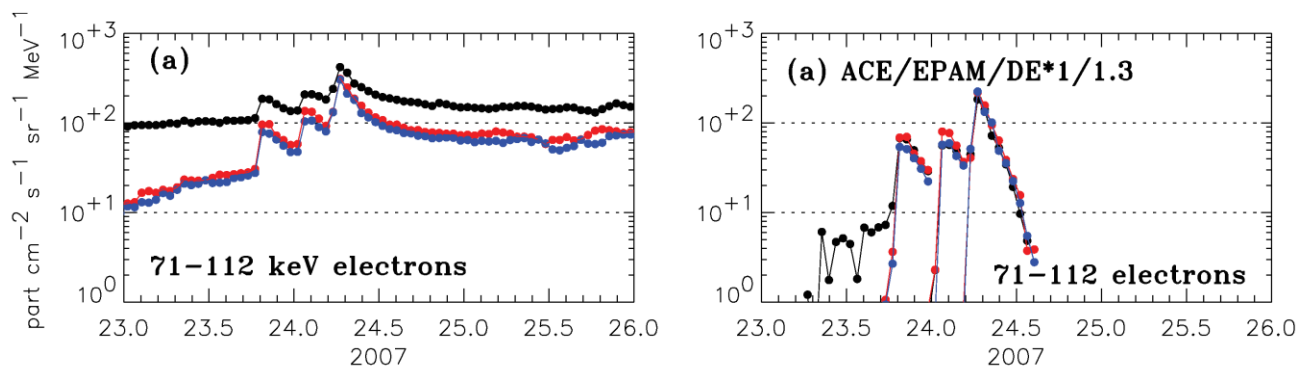


Fig. 1. Time profiles of three consecutive SEP electron events observed by STEREO-B, STEREO-A and ACE during 23-24 January 2007 when all three s/c were close to each other by s/c separation of less than 0.014 AU. **Left panel:** hourly averages of 71-112 keV electron intensity during 23-24 January 2007 events obtained by ACE(EPAM (black), STEREO-A (red)

and STEREO-B (blue). The *right panel* show the same data as the left panel after pre-event intensity subtraction and application of the indicated multiplicative factor.

References

- Mueller-Mellin, R., S. Boettcher, J. Falenski, E. Rode, L. Duvet, T. Sanderson, B. Butler, B. Johlander, and H. Smit, The solar electron and proton telescope for the STEREO mission, 2008, Space Sci. Rev., 136, 363 –389, doi:10.1007/s11214-007-9204-4.
- Lario, D., Aran, A., Gomez-Herrero, R., et al., ApJ, 767, 41